

Optimizing Process Parameters for Increasing Corrosion Resistance of Friction Stir Spot Welded Dissimilar Al-5086/C10100 Joints

S. Siddharth¹  · T. Senthilkumar¹

Received: 6 June 2017 / Accepted: 17 November 2017 / Published online: 7 December 2017
© The Indian Institute of Metals - IIM 2017

Abstract In this paper, dissimilar aluminium Al-5086/C10100 copper spot joints were made using friction stir spot welding, by varying the significant process parameters such as tool rotational speed, plunge depth and dwell time. Using a central composite design model, twenty experiments were conducted and the welded joints were subjected to corrosion analysis. Using electro-chemical system, polarization tests were conducted and salt fog testing was conducted for 20 h. Empirical relationships were established between the process parameters with the pitting potential and the rate of mass loss. ANOVA was used to evaluate the model's significance and optimization was done using response surface methodology. It was observed that, at 1112 rpm of tool speed, 2.07 mm of plunging depth and 12.3 s of dwelling period, most positive pitting potential of -586.86 eV and minimum mass loss of 0.0010234 g occurred. The model was validated with error within three percentage, which indicated high predictability of the developed model.

Keywords Friction stir spot welding · Aluminium · Copper · Corrosion · Optimization

1 Introduction

Friction stir spot welding (FSSW) is a linear modification of the previously patented Friction stir welding process, by The Welding Institute [1]. FSSW is a solid state three step joining process involving plunging, stirring and drawing out. During plunging process, a high speed non-consumable rotating tool is forcibly plunged into the workpieces held in lap configuration. During stirring, for a predefined time duration, the rotating tool is held at the plunged position for inducing frictional stir. In drawing out stage, the tool is pulled out from the weld spot so as to allow the weld zone to cool and re-solidify so as to form as friction stir spot joint [2]. The three step FSSW process is indicated in Fig. 1. Many investigations are being carried out all over the world for joining materials using FSSW process. Manickam and Balasubramanian [3] conducted FSSW experiments on dissimilar combination of Al6061 aluminium and Copper alloy and optimized the process parameters for achieving higher tensile properties. Arul et al. [4] conducted FSSW experiments using Al 5754 plates and observed the failure criteria like necking and shearing. Pan et al. [5] conducted FSSW experiments on 6 series aluminium alloy (Al 6111 alloy), by increasing the plunge depths from 1.6 mm to 1.9 mm and observed the failure modes. In addition to the weld quality, the corrosion aspects of joints should be analysed for understanding the behaviour and lifetime of the joints in volatile environment. Fahimpour et al. [6] analysed the corrosion behaviour of joints of aluminium Al6061 alloy using friction stir welding and gas tungsten arc welding. Weifeng et al. [7] analysed the pitting corrosion behaviour of thick aluminium joints using cyclic polarization techniques and the microstructural modifications due to the effect of alkaline chloride solution using scanning electron microscopy and advanced atomic force microscopy.

✉ S. Siddharth
skmsiddharth1@yahoo.in

T. Senthilkumar
kmtsenthil@gmail.com

¹ Department of Mechanical Engineering, University College of Engineering, Anna University, Tiruchirappalli, Tiruchirappalli 620 024, India

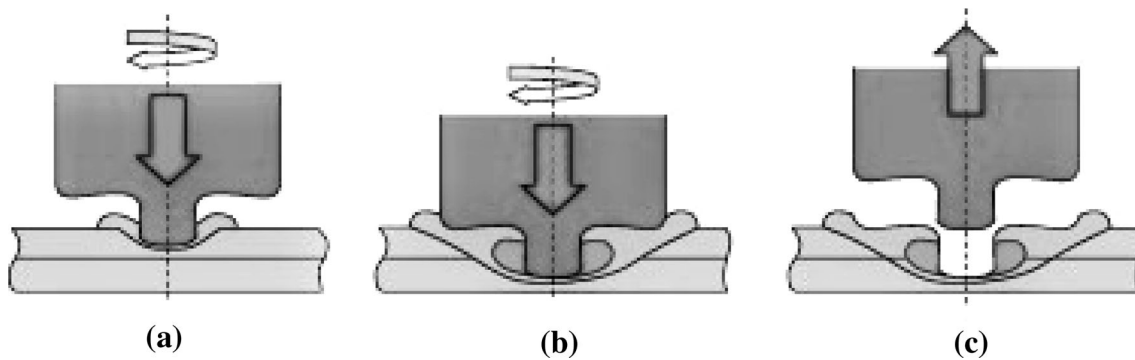


Fig. 1 Friction stir spot welding process. **a** Plunging, **b** stirring, **c** drawing out

Paglia and Buchheit [8] observed the corrosion aspects of friction stir welded aluminium alloys owing to sensitization of the grain microstructures and increased the corrosion resistance by modifying the microchemistry of the friction stir welded joints. Yong et al. [9] evaluated the corrosion aspects of friction stir welded aluminium 7A52 alloy and observed the variation in stress corrosion index due to the changes in cathodic polarization. Chen et al. [10] conducted fatigue tests on 2 series aluminium alloy such as Al2024 at various corrosion environments and evaluated the multiaxial fatigue behaviour with changes in corrosion duration. Reyes-Hernández et al. [11] conducted Gas tungsten arc welding experiments on 2205 duplex steels and observed the variations in corrosion properties when nitrogen atmosphere was used. Liu et al. [12] investigated the corrosion aspects of high strength low alloy steels which were welded by using submerged arc as well as electro-gas (vertically modified) joining technique and found that vertical electro gas welded joints were more resistant to corrosion than submerged arc welded joints. Dick et al. [13] studied the corrosion behaviour of friction stir welded 7 series aluminium alloy such as Al7050 and observed that the pitting resistance was lesser in the nugget zone. From the study of previous investigations, it could be inferred that the research on corrosion aspects of dissimilar Al/Cu welded joints were not found. Thus, in this current investigation, the important friction stir spot welding process parameters were optimized for enhancing the corrosion properties of Al-5086/C10100.

2 Materials and Methods

2.1 Base Material Selection

For this investigation, 5 series aluminium alloy Al-5086-H32 (1.5 mm thick) and rolled Copper C10100 sheet of 1.5 mm thickness, were selected as the base materials. The work pieces were sized to a length of 100 mm, breadth of 30 mm, and the weld surfaces were thoroughly cleaned to remove impurities. An overlap of 30 mm was given for all

the Al/Cu dissimilar lap configuration specimens and Al was placed on the top and Cu was placed at the bottom. The nominal chemical composition of the base materials is indicated in Table 1 and the important mechanical characteristics of the base materials are indicated in Table 2.

2.2 Establishing Feasible Limits and Experimental Details

The sets of dissimilar friction stir spot welding (FSSW) joints were done using a modified heavy type computer numerical controlled vertical milling machine. The equipment is shown in Fig. 2. The cutting tool of the milling machine was replaced with a non-consumable FSSW tool made up of H13 material. The FSSW tool was made with cylindrical straight geometry, having a cylindrical shoulder diameter of 16 mm, cylindrical pin diameter of 6 mm and pin height of 1.5 mm. The FSSW tool is shown in Fig. 3 with its dimensions. The important friction stir spot welding process parameters which influence the weld characteristics were found to be tool rotational speed in rpm, plunge depth in millimetres, the time span of dwelling (dwelling time) in seconds, the axial spindle movement speed in mm/min and the axial force for plunging [14]. From previous literatures and through experimental trials, the three FSSW process parameters were varied while the axial spindle feed was maintained at 18 mm/min so as to eliminate any kind of impact contact between the tool tip and the Al plate and an axial force of 1000 N was maintained for plunging the specimens during the welding process.

The limits of the process parameters were fixed so as to obtain a good weld appearance, appropriate flash and keyhole dimensions. From trial and error experiments, the following observations were made.

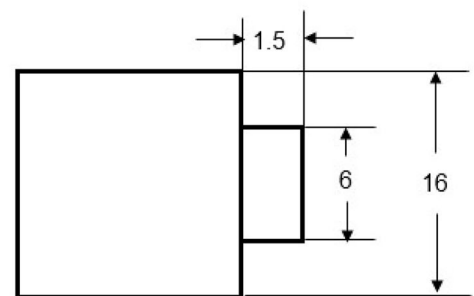
1. When the speed of rotation of non-consumable tool was reduced below 775 rpm, the plunging action was more of a shear, thus resulting in improper joints (Fig. 4a).
2. When the rotational speed of the non-consumable tool was increased beyond 1475 rpm, the stir on the spot

Table 1 Chemical composition of the base materials (wt%)

Base materials	Mg	Si	Mn	Fe	Zn	Ti	Cr	Co	Cu	Al
Al-5086-H32	4.17	0.23	0.57	1.34	0.18	–	0.105	–	0.05	Bal.
	Pb	Sn	S	Fe	Zn	O	P	As	Cu	
C10100	0.003	0.002	0.004	0.004	0.003	0.002	0.002	0.002	Bal	

Table 2 Important mechanical properties of the base materials

Base materials	Melting point °C (solidus)	Density (g/cm ³)	Ultimate tensile strength (MPa)	Yield strength (MPa)	Elongation (%)	Hardness (HV)
Al-5086-H32	585	2.66	290	207	12	88
Cu C10100	1083	8.94	320	285	20	82

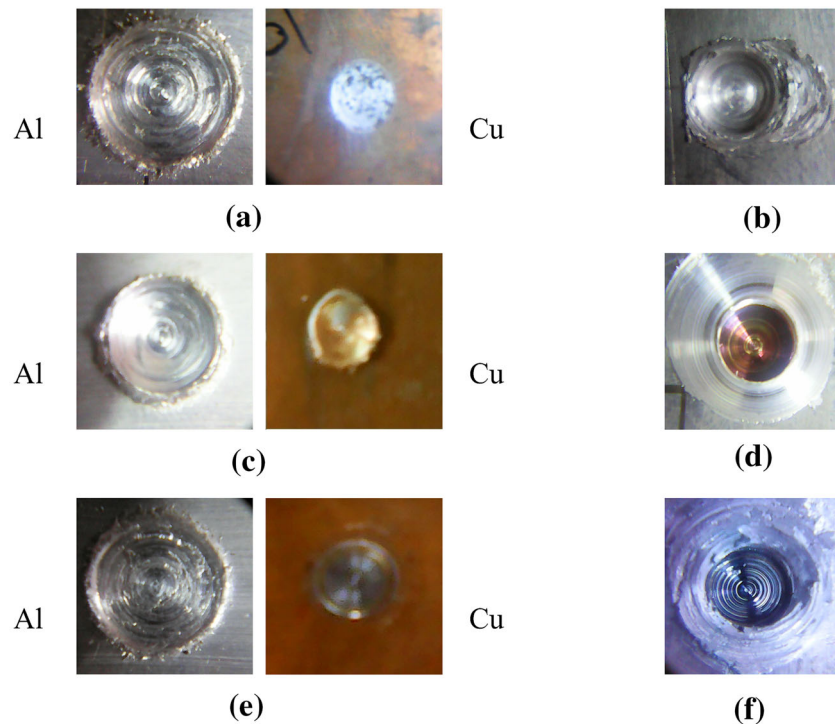
**Fig. 2** Equipment used for friction stir spot welding experiments**Fig. 3** Friction stir spot welding tool

All dimensions are in millimeters

resulted in excessive melting resulting in defective joints (Fig. 4b).

3. If the duration of dwell time was lesser than 8 s, the time duration was not sufficient to stir and soften the top and bottom plates. This resulted in improper spot joints (Fig. 4c).
4. When the dwell time duration was increased beyond 15 s, excessive stirring resulted in melting of the weld region, and sticking of top plate to the tool and bottom plate to the fixture occurred, thereby resulting in erroneous joint (Fig. 4d).
5. If the depth of piercing of the tool was lesser than 1.6 mm, the bottom plate was not softened enough to enable fusion and intermixing of the top and bottom components, to ensure a proper joint (Fig. 4e).
6. If the depth of piercing was maintained above 2.6 mm, the extent of keyhole produced was enormous and excessive lash reduced the amount of softened material within the weld spot, thereby producing defective welds (Fig. 4f).

Fig. 4 Pictures of joints fabricated beyond feasible limits. **a** Tool rotational speed < 775 rpm, **b** tool rotational speed > 1475 rpm, **c** dwell time < 8 s, **d** dwell time > 15 s, **e** plunge depth < 1.6 mm, **f** plunge depth > 2.75 mm



The range of the process parameter values are indicated in Table 3. Using a software based electro-chemical system (Gill AC type), polarization tests were conducted by incorporating the potentiodynamic method, for evaluating the pitting corrosion aspects of the welds. For reference electrode, a saturated calomel electrode was used and for auxiliary, carbon electrodes were used. 3.5% aerated NaCl solution was used for conducting the corrosion tests. The pH value of the solution was maintained at 10, by addition of potassium hydroxide. At 0.166 mV/s the potential scanning was done with -0.25 (OC—Saturated Calomel Electrode) as the initial potential till the final pitting potential value. The equipment is shown in Fig. 5.

Using salt fogging testing equipment, the corrosion aspects of the welded zone of dissimilar friction stir spot welded Al-5086/C10100 joints were studied. The apparatus setup is indicated in Fig. 6. The equipment comprised of a closed chamber made up of glass and contains square shaped rods made up of plastic for the specimens to be tied and arranged. A nozzle for the flow of air and another

nozzle for flow of water were used inside the enclosed equipment. An air compressor was connected to the air nozzle, a container comprising of NaCl solution was connected to the water nozzle. The air compressor was used for supplying working air inside the chamber at the required pressure. The two nozzles were made to be situated 90° apart from each other so as to create NaCl fog inside the chamber.

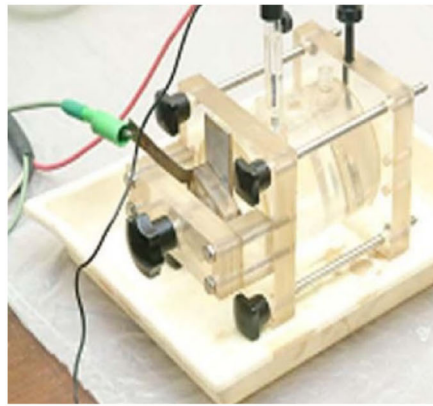
2.3 Central Composite Design Model Development

A central composite design model was selected as the individual factor value ranges were found to be high. 20 sets of coded conditions were obtained. With 8 points, a five-level central composite design model was used, with six star and central points. The most positive value was coded as $+1.682$ and the most negative value was coded to be -1.682 . The intermediate range of the values were obtained using the relationship compiled by Montgomery [15]

Table 3 Range of friction stir spot welding process parameter values for Al-5086/C10100 joints

No.	Parameter	Notation	Unit	Levels				
				- 1.68	- 1	0	1	+ 1.68
1	Tool rotation speed	TRS	rpm	775	916	1125	1333	1475
2	Dwell time	DT	s	8	9.5	11.5	13.5	15
3	Plunge depth	PD	mm	1.6	1.8	2.1	2.4	2.6

Fig. 5 Electro-chemical equipment for potentio-dynamic polarization study



Electro-chemical equipment



Data processing system

Fig. 6 Salt spray fog apparatus used for corrosion analysis



$$W_i = 1.682 [2W - (W_{\max} + W_{\min}) / (W_{\max} + W_{\min})] \quad (1)$$

In the above given equation, the value of the coded variable W is W_i . From W_{\min} to W_{\max} , W is made to assume any variable value. The least value is taken as W_{\min} and W_{\max} is termed to be the highest value. The central composite design matrix formed with the twenty conditions are indicated in Table 4.

Twenty sets of dissimilar joints were fabricated with the process parameter values indicated in Table 4. A few of the joints fabricated are indicated in Fig. 7.

3 Results and Discussion

3.1 Establishing Empirical Relationships and ANOVA Analysis

The corrosion specimens were placed in the flat cell by using a shoe assembly which can be adjusted to appropriately expose the specimens to the solution. 250 ml of the

testing solution was poured into the flat cell and with the help of the leads from the cell, the three electrodes were joined to the corrosion equipment. An electrical contact was established between the back surface of the specimen and the shoe which were held at position using a gasket made up of Teflon. With 1 cm^2 exposure area, the corrosion experiments were conducted. The critical value of the pitting potential was termed as the potential at which the value of current increased suddenly to a higher value. The joints that tends to exhibit positive potential or low negative potential values were termed to have a higher pitting resistance. The pitting initiation could be attributed to the presence of intermetallics at the weld regions [16]. The galvanic couple formation within the intermetallic components and the nearby matrix was attributed to the dissolution of the localized matrix [17]. The E_{pit} values of the welded region of the dissimilar twenty Al/Cu combinations are represented in Table 4.

In salt spray apparatus, using a non-corrosive thread made up of polymer based material, the weld specimens were tied so that they were held at angles varying from 7° to 15° parallelly, to the direction of flow of the fog from the

Table 4 Central composite design matrix and experimental results

No Run	Coded factor value			Actual factor value			Pitting E_{pit} (mV)	Mass loss in grams
	TRS	DT	PD	TRS rpm	DT s	PD mm		
1	0	- 1.68	0	1125.00	8.00	2.10	- 631	0.00197754
2	- 1	- 1	- 1	916.89	9.42	1.80	- 685	0.00221987
3	+ 1	- 1	+ 1	1333.11	9.42	2.40	- 561	0.00223995
4	0	0	0	1125.00	11.50	2.10	- 588	0.00097399
5	0	0	0	1125.00	11.50	2.10	- 585	0.00101418
6	0	+ 1.68	0	1125.00	15.00	2.10	- 603	0.00155674
7	0	0	- 1.68	1125.00	11.50	1.60	- 648	0.00143617
8	0	0	0	1125.00	11.50	2.10	- 587	0.00113475
9	- 1	- 1	+ 1	916.89	9.42	2.40	- 626	0.00191854
10	+ 1.68	0	0	1475.00	11.50	2.10	- 595	0.00215957
11	+ 1	+ 1	+ 1	1333.11	13.58	2.40	- 612	0.00230024
12	0	0	0	1125.00	11.50	2.10	- 591	0.00109456
13	+ 1	- 1	- 1	1333.11	9.42	1.80	- 636	0.00185816
14	0	0	+ 1.68	1125.00	11.50	2.60	- 592	0.00213948
15	- 1	+ 1	- 1	916.89	13.58	1.80	- 596	0.00147686
16	0	0	0	1125.00	11.50	2.10	- 587	0.00111466
17	+ 1	+ 1	- 1	1333.11	13.58	1.80	- 625	0.00141608
18	0	0	0	1125.00	11.50	2.10	- 586	0.00107447
19	- 1	+ 1	+1	916.89	13.58	2.40	- 603	0.00175851
20	- 1.68	0	0	775.00	11.50	2.10	- 625	0.00195863

**Fig. 7** Pictograph of friction stir spot welding joints

nozzles. At a consistent flow, the NaCl droplets were made to come in contact with the specimens. For 20 h, the experiment was conducted and the weight loss was calculated at the end. After completion of test, the specimens were thoroughly rinsed and dried after which it was

weighed. The variations in weight loss were recorded and are indicated in Table 4.

The responses were recorded in the form of Pitting potential E_{pit} and mass loss in grams, were correlated to be functions of the three friction stir spot welding process parameters. The relationship is indicated as per the procedures used by Paventhan et al. [18].

$$\text{Pitting potential } E_{\text{pit}} \text{ in electro chemical corrosion test} \\ = f\{\text{TRS, DT, PD}\} \quad (2)$$

$$\text{Mass loss in grams in salt spray test} = f\{\text{TRS, DT, PD}\} \quad (3)$$

The response surface two models of pitting potential and mass loss is represented to be a polynomial regression equation of second order [15]

$$T = a_0 + \sum a_i x_i + \sum a_{ii} x_i^2 + \sum a_{ij} x_i x_j \quad (4)$$

For the process parameters such as tool rotational speed in the form of (TRS), dwelling time (DT) and depth of plunging (PD), the expression of the polynomial can be given as

Pitting potential/Mass loss

$$= \{a_0 + a_1 \text{ TRS} + a_2 \text{ DT} + a_3 \text{ PD} + a_{12} \text{ TRS} * \text{ DT} + a_{13} \text{ TRS} * \text{ PD} + a_{23} \text{ DT} * \text{ PD} + a_{11} \text{ TRS}^2 + a_{22} \text{ DT}^2 + a_{33} \text{ PD}^2\} \tag{5}$$

a_0 is determined to be the average of all the responses. a_1, a_2, \dots , are termed as other coefficients of regression which correlates to linear, squared and interaction terms of factor components [18]. By using design expert software, coefficients of significance were evaluated by following student’s t test. For evaluating the significance of the developed model, ANOVA analysis was conducted. The ANOVA analysis result of pitting potential variations are indicated in Table 5 and ANOVA results of response model of mass loss in salt spray test is shown in Table 6.

The values of “Prob > F” at lesser than 0.005, showed a clear indication that the model terms were at a high level of significance. Wherever the values were found to be greater than 0.10, the model terms were observed to be insignificant. The coefficients were incorporated for development for empirical relationships for the predicted pitting potential and mass loss.

Pitting potential

$$= -587.31 + 9.26 \text{ TRS} + 8.72 \text{ DT} + 17.15 \text{ PD} - 19 \text{ TRS} * \text{ DT} + 4.5 \text{ TRS} * \text{ PD} - 16 \text{ PD} * \text{ DT} - 8.14 \text{ TRS}^2 - 10.62 \text{ DT}^2 - 11.68 \text{ PD}^2 \tag{6}$$

$$\begin{aligned} \text{Mass loss} = & +1.068 \times 10^{-03} + 5.701 \times 10^{-05} \text{ TRS} \\ & - 1.459 \times 10^{-04} \text{ DT} + 1.779 \times 10^{-04} \text{ PD} \\ & + 6.516 \times 10^{-05} \text{ TRS} * \text{ DT} + 1.607 \\ & \times 10^{-04} \text{ TRS} * \text{ PD} + 1.357 \times 10^{-04} \text{ DT} * \text{ PD} \\ & + 3.459 \times 10^{-04} \text{ TRS}^2 + 2.427 \times 10^{-04} \text{ DT}^2 \\ & + 2.500 \times 10^{-04} \text{ PD}^2 \end{aligned} \tag{7}$$

The fitted values are indicated in Tables 5 and 6 using ANOVA analysis. The determination coefficient was R^2 . For identification of the goodness of fit for the developed model, the determination coefficient was used. From the two developed models, it could be inferred that only five percent was left unexplained [19]. As the adjusted value of the determination coefficient was high, the significance of the developed model was attributed to be high. An acceptable level of agreement was found between the adjusted determination coefficient value and the predicted R^2 value. Figure 8a shows the correlation between the predicted and actual values of pitting potential (E_{pit}) values and Fig. 7b shows that for mass loss in grams.

By using analytical techniques and mathematical strategies, the correlation between the three-vital friction stir spot welding process parameters with the pitting potential and mass loss were evaluated.

3.2 Optimization Using Response Surface Methodology

Response surface methodology, a statistical and mathematical analytic technique was used to perform the

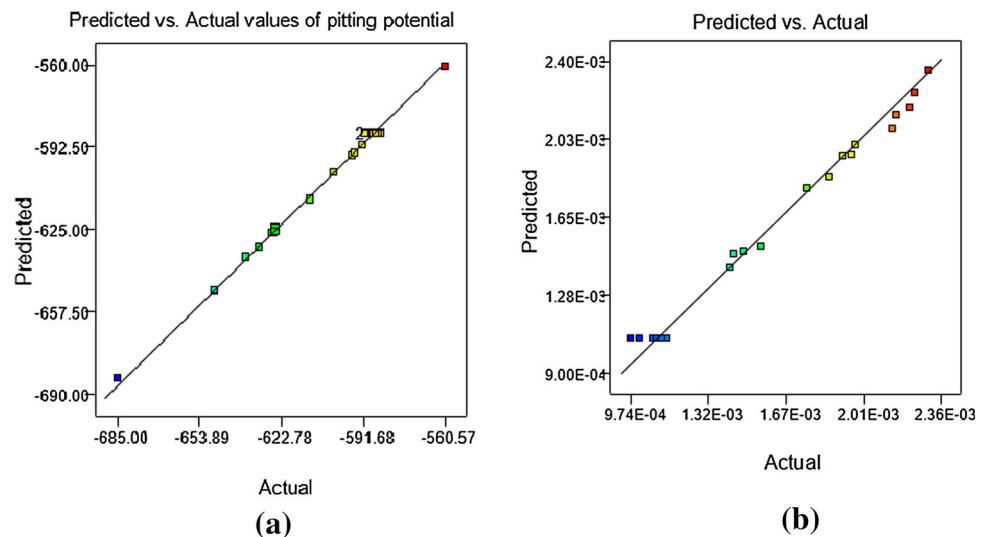
Table 5 Results of ANOVA analysis of pitting potential model

Source	Sum of squares (SS)	DOF	Mean square (MS)	F value	p value Prob > F	Note
Model	15,142.23	9	1682.47	568.96	< 0.0001	Significant
TRS	1170.88	1	1170.88	395.96	< 0.0001	
DT	1038.49	1	1038.49	351.19	< 0.0001	
PD	4015.60	1	4015.60	1357.96	< 0.0001	
TRS DT	2888.00	1	2888.00	976.64	< 0.0001	
TRS PD	162.00	1	162.00	54.78	< 0.0001	
DT PD	2048.00	1	2048.00	692.57	< 0.0001	
TRS ²	955.73	1	955.73	323.20	< 0.0001	
DT ²	1624.89	1	1624.89	549.49	< 0.0001	
PD ²	1965.72	1	1965.72	664.75	< 0.0001	
Residual	29.57	10	2.96			
Lack of fit	8.24	5	1.65		0.8402	Not significant
SD		1.72		R^2	0.9981	
Mean		- 608.10		Adj R^2	0.9963	
C.V. %		0.28		Pred R^2	0.9936	
PRESS		96.36		Adeq precision	101.002	

Table 6 Results of ANOVA analysis of salt spray corrosion mass loss model

Source	Sum of squares (SS)	DOF	Mean square (MS)	F value	<i>p</i> value Prob > F	Note
Model	4.080×10^{-06}	9	4.534×10^{-07}	129.24	< 0.0001	Significant
TRS	4.439×10^{-08}	1	4.439×10^{-08}	12.65	0.0052	
DT	2.907×10^{-07}	1	2.907×10^{-07}	82.88	< 0.0001	
PD	4.321×10^{-07}	1	4.321×10^{-07}	123.17	< 0.0001	
TRS DT	3.396×10^{-08}	1	3.396×10^{-08}	9.68	0.0110	
TRS PD	2.066×10^{-07}	1	2.066×10^{-07}	58.90	< 0.0001	
DT PD	1.472×10^{-07}	1	1.472×10^{-07}	41.98	< 0.0001	
TRS ²	1.725×10^{-06}	1	1.725×10^{-06}	491.66	< 0.0001	
DT ²	8.490×10^{-07}	1	8.490×10^{-07}	242.02	< 0.0001	
PD ²	9.009×10^{-07}	1	9.009×10^{-07}	256.83	< 0.0001	
Residual	3.508×10^{-08}	10	3.508×10^{-09}			
Lack of fit	1.596×10^{-08}	5	3.193×10^{-09}		0.5759	Not significant
SD		5.923×10^{-05}		R ²	0.9915	
Mean		1.641×10^{-03}		Adj R ²	0.9838	
C.V. %		3.61		Pred R ²	0.9636	
PRESS		1.500×10^{-07}		Adeq precision	30.783	

Fig. 8 Scatter diagram indicating the relationship between the actual and predicted values of responses. **a** Predicted versus actual pitting potential, **b** predicted versus actual mass loss



optimization. For attaining the required dependent variable, the independent variable process parameters (factors in this case) were evaluated by this methodology.

Quantitative representation of the independent factors are as follows

$$K = \Phi(X_1, X_2, \dots, X_k) + er \quad (8)$$

K is termed to be the response. The quantitative factors are X_1, X_2, \dots . Φ is the response surface of that equation. *er* is error reduction during the process of experimentation. For a set of two independent variables, its appropriate response surface is developed. In certain cases where the exact value of Φ is unknown, by approximation within the

experimental domain, its value is approximated. The higher the degree of the polynomial, the clarity of correlation gets higher, but there will be higher expenditure involved in experimentation [19].

In this analysis, response surface methodology was used for improving the corrosion properties of the dissimilar Al-5086/C10100 joints in terms of increasing the pitting potential in pitting corrosion tests and reducing the rate of mass loss during salt spray test, with a proper combination of the three-process parameter variable value. The three process parameters such as TRS, PD and DT were formed to be the surface to which fitting of appropriate mathematical model was done.

The variations in responses were indicated clearly by using contours, as circular geometric diagrams for indicating the interdependence of the three input variables. Visual indication of the optimality region was obtained. For first order models, the contour patterns were simple but the complexity of the contours increased for higher order models. The characterization of response surface was done within the vicinity of the stationary spot. Three types of stationary point characterization was done such as maximum, minimum or saddle point. The point was characterized upon evaluating the contour plots, which were generated by using design expert software. Identification of the optimal values was done after characterization. Independence of the factors was seen in circular contour shapes and elliptical shapes indicating factor interactions [19].

Two of the process parameter values were selected at the middle range and they were plotted in the two-dimensional axis and the responses in the form of pitting potential and mass loss in grams were traced.

The optimal point is identified from surface plots. The contours and surface plots for the developed pitting potential model is indicated in Fig. 9 and that for the corrosion rate of mass loss model is shown in Fig. 10. For pitting potential maximization model, Fig. 9a shows the contour plot of TRS versus DT, Fig. 9b indicates the contour diagram of TRS versus PD, Fig. 9c indicates the contour plot of DT versus PD for the optimization model of the dissimilar Al-5086/C10100 joints. Figure 9d shows 3D surface plot for TRS versus DT, Fig. 9e shows the surface plots for PD versus TRS and Fig. 9f shows the surface plot for PD versus DT.

For immersion test mass loss minimization model, Fig. 10a shows the contour plot of TRS versus DT, Fig. 10b indicates the contour diagram of TRS versus PD, Fig. 10c indicates the contour plot of DT versus PD for the optimization model of the dissimilar Al-5086/C10100 joints. Figure 10d shows 3D surface plot for TRS versus DT, Fig. 10e shows the surface plots for PD versus TRS and Fig. 10f shows the surface plot for PD versus DT.

After analysing the contours and surface plots, it was observed that for an initial increase of process parameter values, the pitting potential (E_{pit}) values increased towards positive and beyond a certain extent, the E_{pit} values started decreasing. Also, the rate of mass loss was found to decrease initially during increase in the process parameter values for a certain extent and beyond a certain limit, the mass loss started to increase. The most positive and the highest possible pitting potential E_{pit} value of -586.86 eV and minimum possible mass loss of 0.0010234 g was observed. The corresponding optimized values of process parameters were tool speed of 1112 rpm, dwell duration of 12.3 s and plunge depth of 2.07 mm.

3.3 Interaction and Perturbation Plots

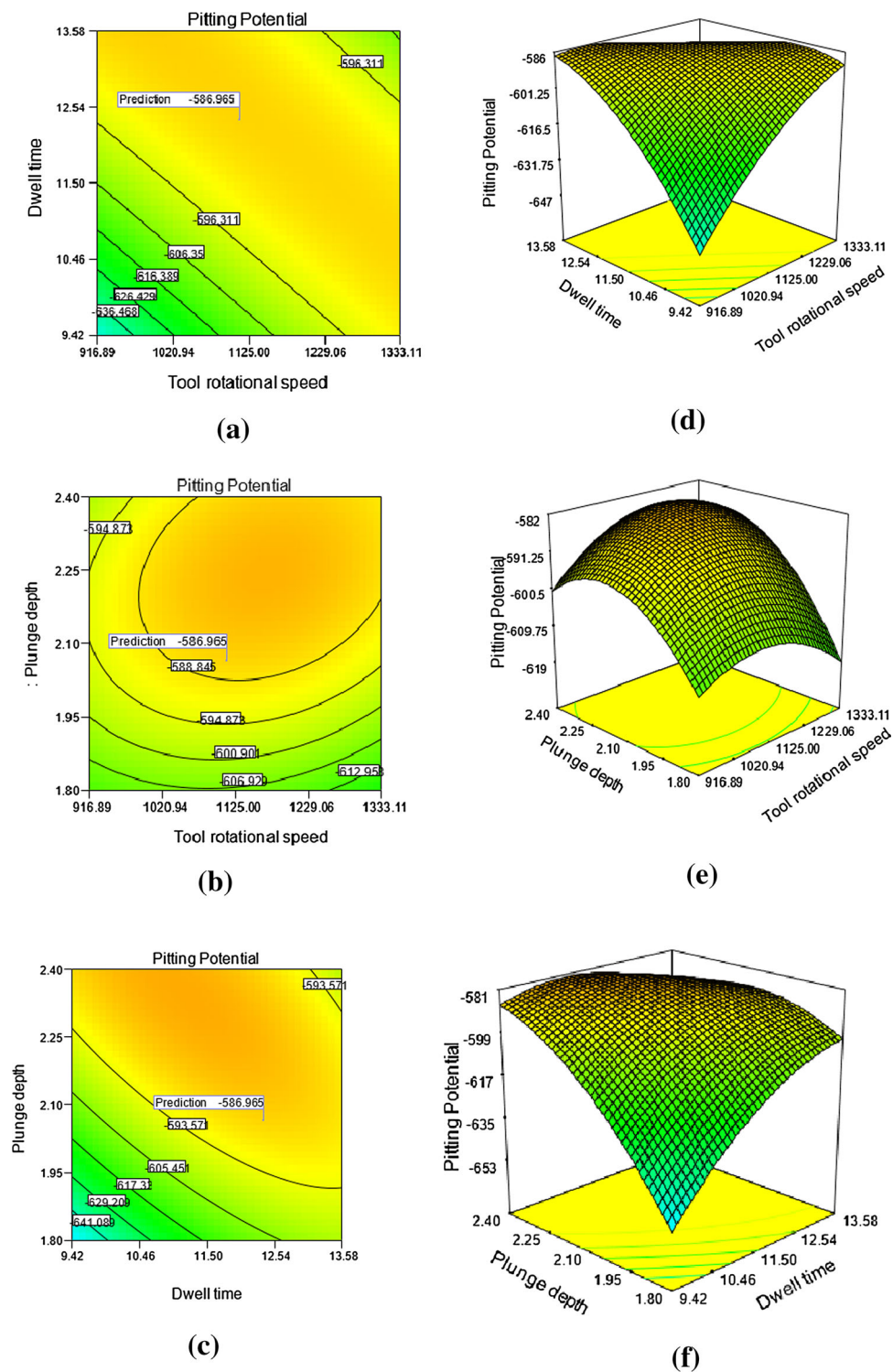
For identifying the effects of changes in the friction stir spot welding process parameters on the corrosion properties of the joints, their interactions were analysed. Lakshminarayanan et al. [14], observed that study of interaction effect of three important friction stir spot welding process parameters such as tool rotational speed, plunge depth and dwell time were important as they influenced the joint quality. Figure 11a indicates the interaction effect of tool rotational speed and dwell time on pitting potential at plunge depth of 2.10 mm. Figure 11b shows the interaction effect of dwell time and plunge depth at tool rotational speed of 990 rpm. Figure 11c shows the perturbation plot indicating the effect of process parameters on changes in pitting potential value. It was observed that plunge depth had a greater influence than tool rotational speed and dwell time.

For corrosion mass loss variation, Fig. 11d indicates the interaction effect of plunge depth and dwell time at tool rotational speed of 990 rpm. Figure 11e shows the interaction effect of plunge depth and tool rotational speed at dwell time of 10.4 s. Figure 11f shows the perturbation plots indicating the effect of variations in friction stir spot welding process parameters on the variation in mass loss due to corrosion. It could be observed that variations in plunge depth had a greater influence than the other two process parameters on mass loss due to corrosion.

3.4 Evaluation of Microstructure

For understanding the effect of corrosion on the welded joints, microstructural analysis was conducted using scanning electron microscopy (SEM—Oxford Instruments TESCAN equipped with VEGA3). The microstructure of welded region of a corroded sample, fabricated with optimized value of friction stir spot welding process parameters was observed and is shown in Fig. 12. Figure 12a–c indicates the microstructure of corroded weld region near the nugget centre at $100\times$ magnification. Figure 12a indicates the corroded regions which can be identified with the difference in the pit density. Voids were observed to be affected due to corrosion, which were found in form of dark spots. Figure 12b shows a less corroded region, wherein corrosion was found near the cracked regions. Figure 12c indicates the occurrence of corrosion at higher concentration along cracks. The occurrence of cracks was minimized owing to the effective stir of the pin portion of the tool and higher intermixing of the softened materials. Figure 12d–f indicates the microstructure of the corroded weld region near the shoulder periphery, at $50\times$ magnification. Figure 12d shows eruptions and occurrence of corrosion under the erupted material. In Fig. 12e, the

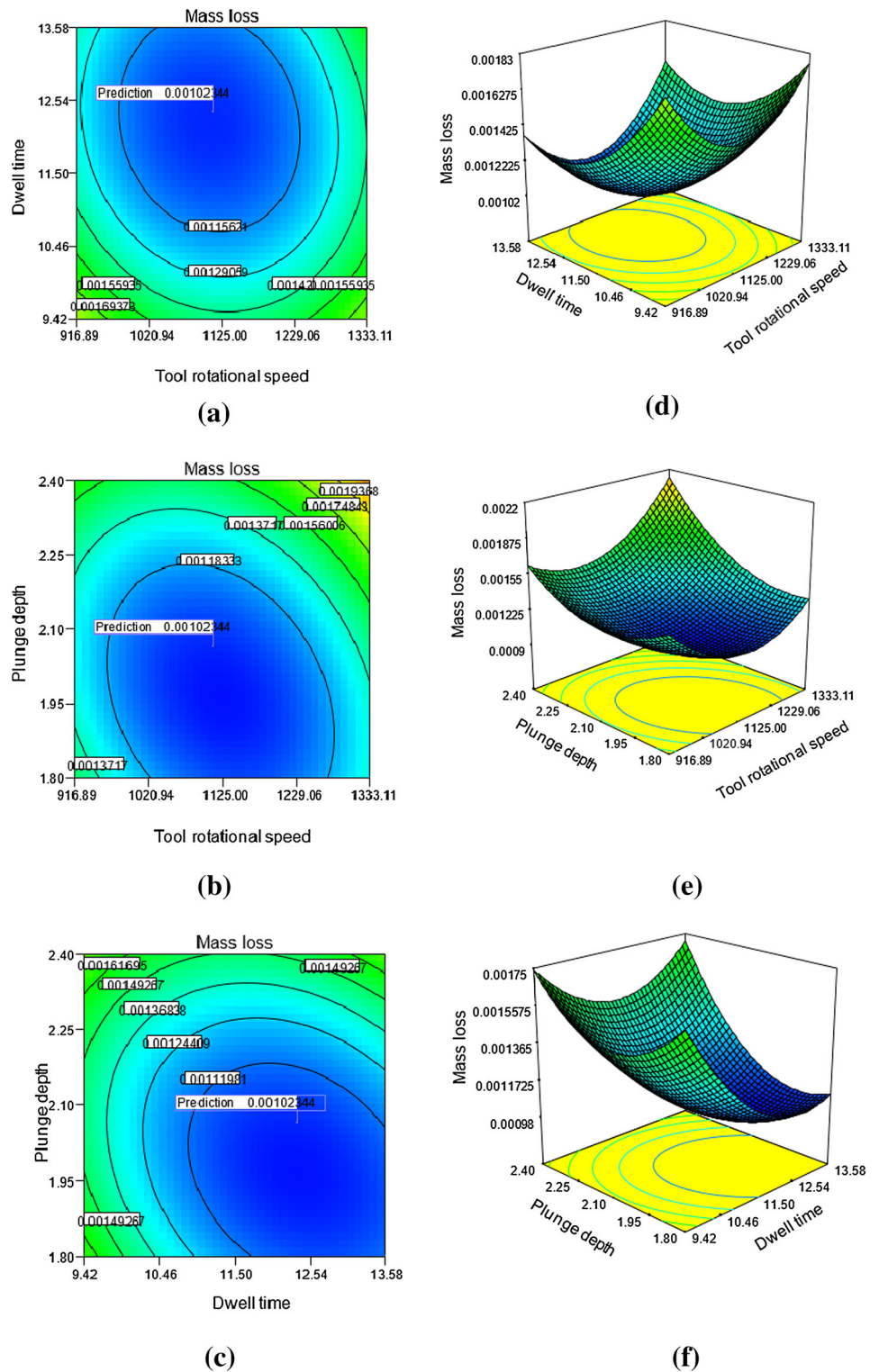
Fig. 9 Contours and surface plots for pitting potential maximization model. **a** Contour plot DT versus TRS, **b** contour plot PD versus TRS, **c** contour plot PD versus DT, **d** surface plot DT versus TRS, **e** surface plot PD versus TRS, **f** surface plot PD versus DT



difference in corrosion density at cracked regions can be observed. Figure 12f shows flake like eruptions and cracks which have higher susceptibility for corrosion. The effect of flash component arising during the plunging action of the tool affects the weld structure at the periphery. Due to the push of the material from centre to periphery and owing

to the variation in the re-solidification pattern along the vertical and horizontal, occurrences of cracks at the weld periphery was found to be more pronounced.

Fig. 10 Contours and surface plots for mass loss in corrosion minimization model. **a** Contour plot DT versus TRS, **b** contour plot PD versus TRS, **c** contour plot PD versus DT, **d** surface plot DT versus TRS, **e** surface plot PD versus TRS, **f** surface plot PD versus DT



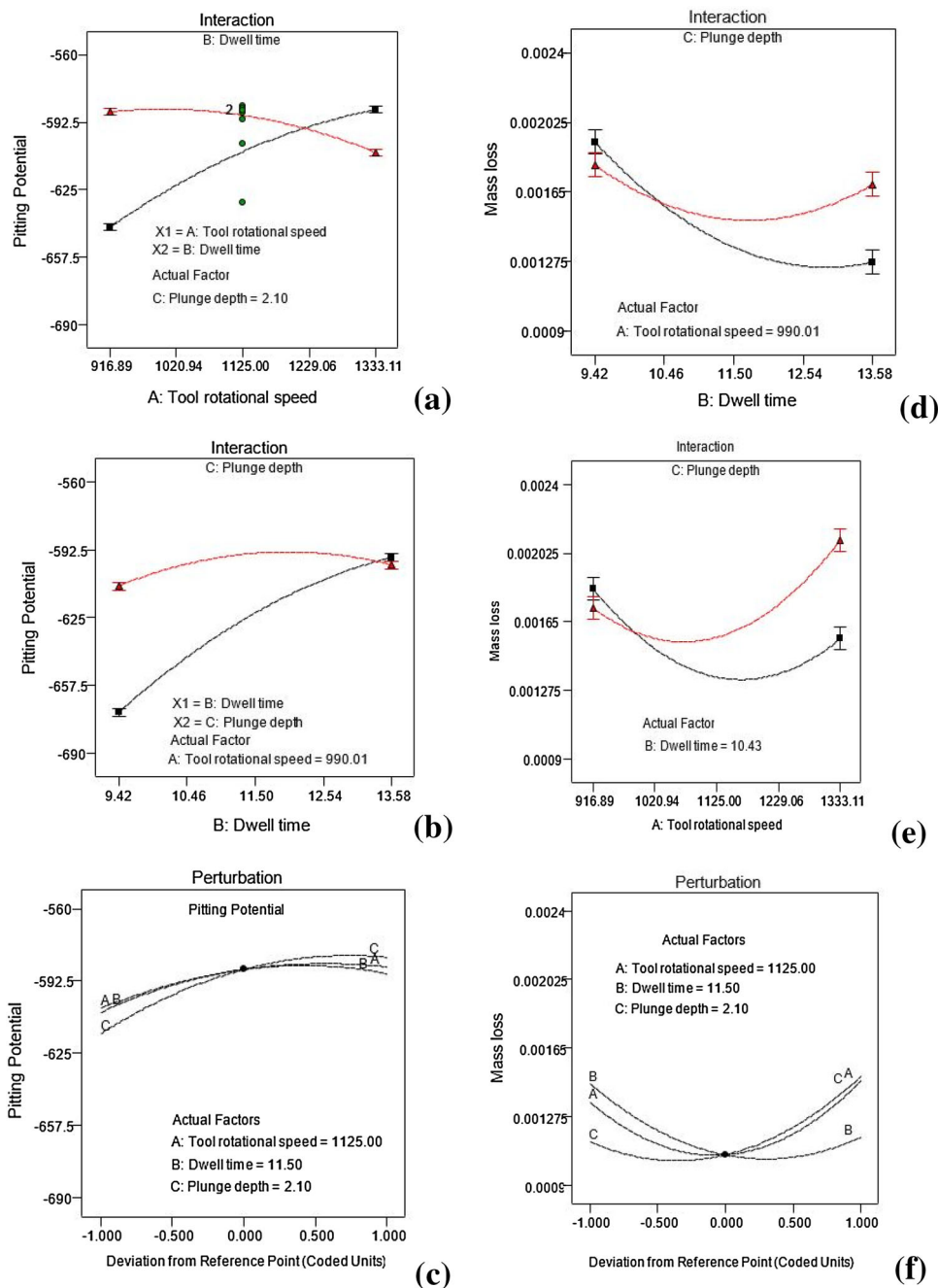
3.5 Validation of Developed Model

For the purpose of validation of the developed model, three more experiments were conducted with the optimized

values of the process parameters and the results are indicated in Table 7.

From validation experiments, it was observed that the difference in error percentage of the predicted and actual pitting potential and mass loss was lesser than three. Thus,

Fig. 11 Interaction and perturbation plots



it could be inferred that the optimization model was developed with very high predictability.

4 Conclusions

Thus, dissimilar friction stir spot welding of Al-5086/C10100 joints were fabricated and were subjected to two types of corrosion tests such as potentiodynamic electro-

chemical pitting test and salt spray test. Using a central composite design model, empirical relationships were developed between the three process parameters such as tool rotational speed, dwell time and plunge depth with pitting potential and mass loss in salt spray test. Using response surface methodology, the optimized set of process parameters for obtaining maximum positive pitting potential value of -586.86 eV and minimum possible mass loss of 0.0010234 g was observed were found to be tool speed

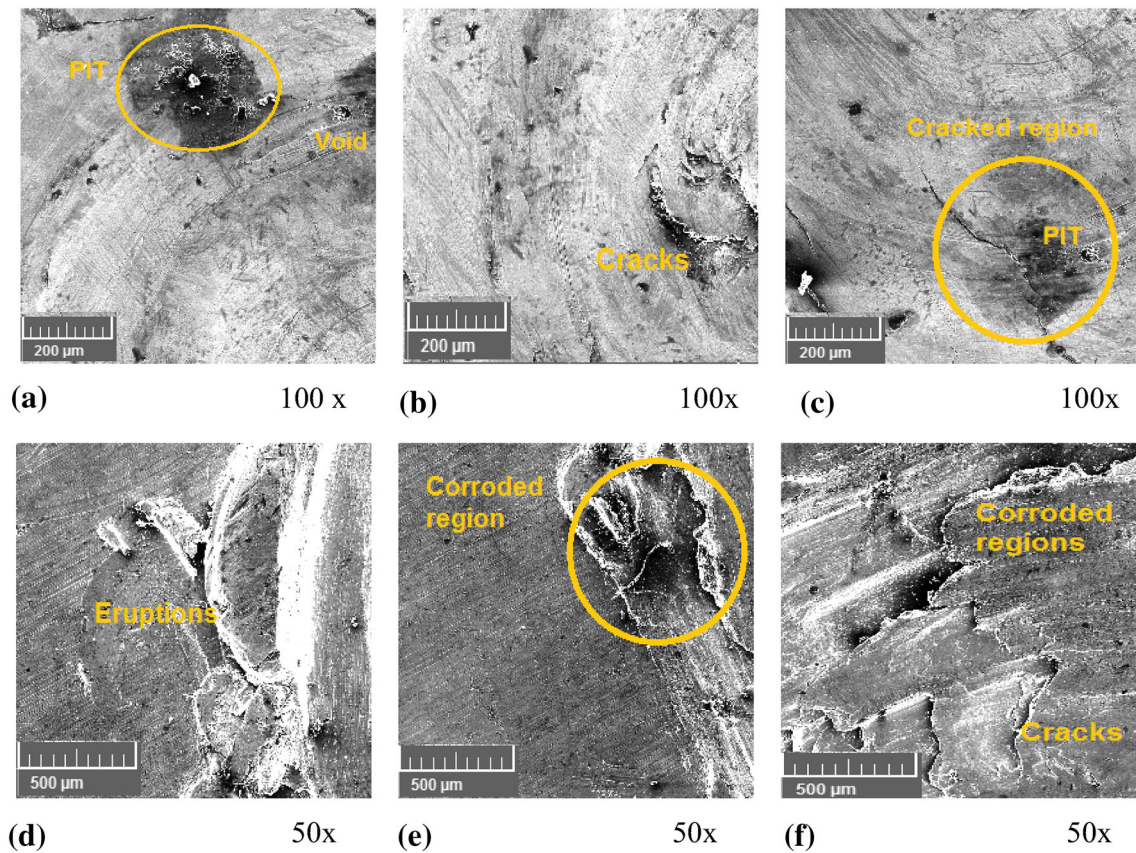


Fig. 12 Microstructural evaluation of corrosion tested specimen. **a** × 100, **b** × 100, **c** × 100, **d** × 50, **e** × 50, **f** × 50

Table 7 Validation experiments and results

Exp no.	Predicted	Experimental	Error %
Pitting potential E_{pit} (mV)			
1	- 586	- 599	- 2.2
2		- 583	+ 1.3
3		- 591	- 1.7
Mass loss in grams			
1	0.0010234	0.0010293	0.57
2		0.0010146	0.85
3		0.0010311	0.75

of 1112 rpm, dwell duration of 12.3 s and plunge depth of 2.07 mm, which were validated within an error of three percentage. From interaction and perturbation plots, among the friction stir spot welding process parameters, variations in plunge depth was found to affect the corrosion aspects of the joints to a greater extent than tool rotational speed and dwell time. Microstructural evaluation indicated occurrence of higher corrosion at cracked regions.

References

1. Thomas W M, Nicholas E D, Needham J C, Murch M G, Temple Smith P, and Dawas C J, *Friction Stir Welding*. International Patent Application No. PCT/GB92/02203 G (1991).
2. Badarinarayan H, *Fundamentals of Friction Stir Spot Welding*, Ph D Thesis, Missouri University (2009).
3. Manickam S, and Balasubramanian V, *J Manuf Eng* **10** (2015) 207.
4. Arul S G, Pan T, Lin P C, Pan J, Feng Z, and Santella M L, *Proceeding of 2005 SAE World Congress*, Detroit, MI (2005).
5. Pan T Y, Joaquin A, Wilkosz D E, Reatheford L, Nicholson J M, Feng Z, and Santella M L, *5th International Symposium on Friction Stir Welding*, TWI, Metz (2004).

6. Fahimpour V, Sadrnezhad S K, and Karimzadeh F, *Mater Des* **39** (2012) 329.
7. Weifeng X, Jnhe L, and Hongqiang Z, *Electrochim Acta*, **55** (2010) 2918.
8. Paglia C S, and Buchheit R G, *Scr Mater* **58** (2008) 383.
9. Yong Gui Y, Li M, Jie Z H, and Bing Z H, *Corros Sci Prot Technol*, **21** (2009) 119.
10. Chen Y, Liu C, Zhou J, and Wang X, *Int J Fatigue*, **98** (2017) 269.
11. Reyes Hernández D, Manzano Ramírez A, Encinas A, Sánchez Cabrera V M, Marroquín De Jesús A, García García R, Orozco G, and Olivares Ramírez J M, *Fuel*, **198** (2017) 165.
12. Liu W, Pan H, Li L, Lv H, Wu Z, Cao F, and Zhu J, *J Manuf Process*, **25** (2017) 418.
13. Dick P A, Knörnschild G H, and Dick L F P, *Corros Sci*, **114** (2017) 28.
14. Lakshminarayanan A K, Annamalai V E, and Elangovan K, *J Mater Res Technol*, **4** (2015) 262.
15. Montgomery D C, *Design and Analysis of Experiments*, John Wiley & Sons, New York (2001).
16. Venkata Rao C, Madhusudhan Reddy G, and Srinivasa Rao K, *Def Technol*, **11** (2015) 123.
17. Srinivasa Rao K, and Prasad Rao K, *Trans Indian Inst Met*, **576** (2004), 593.
18. Paventhan R, Lakshminarayanan P R, and Balasubramanian V, *Trans Nonferrous Met Soc China* **21** (2011) 1480.
19. Miller J E F, and Johnson R, *Probability and Statistics for Engineers*, 5, Prentice Hall, New Delhi (1996).